



HAL
open science

Probabilistic downscaling of GCM scenarios over southern India

Nicolas Vigaud, M. Vrac, Yvan Caballero

► **To cite this version:**

Nicolas Vigaud, M. Vrac, Yvan Caballero. Probabilistic downscaling of GCM scenarios over southern India. *International Journal of Climatology*, 2013, 33 (5), pp.1248-1263. 10.1002/joc.3509 . hal-02986860

HAL Id: hal-02986860

<https://brgm.hal.science/hal-02986860>

Submitted on 3 Nov 2020

HAL is a multi-disciplinary open access archive for the deposit and dissemination of scientific research documents, whether they are published or not. The documents may come from teaching and research institutions in France or abroad, or from public or private research centers.

L'archive ouverte pluridisciplinaire **HAL**, est destinée au dépôt et à la diffusion de documents scientifiques de niveau recherche, publiés ou non, émanant des établissements d'enseignement et de recherche français ou étrangers, des laboratoires publics ou privés.

ABSTRACT: The cumulative distribution function transform (CDF-t) is used to downscale daily precipitation and surface temperatures from a set of Global climate model (GCM) climatic projections over southern India. To deal with the annual cycle, the approach has been applied by months, allowing downscaled projections for all seasons. First, CDF-t is validated over a historical period using observation from the Indian Meteorological Department (IMD). Resulting high-resolution fields show substantial improvements compared to original GCM outputs in terms of distribution, seasonal cycle and monsoon means for arid, semi-arid and wetter regions of the subcontinent. Then, CDF-t is applied to GCM large-scale fields to project rainfall and surface temperature changes for the 21st century under the IPCC SRES A2 scenario. The results obtained show an increase of rainfall, mostly during the monsoon season, while winter precipitation is reduced, suggesting a widespread warming especially in the winter and post-monsoon season. Copyright © 2012 Royal Meteorological Society

KEY WORDS downscaling; climatic scenarios; southern India

Received 14 June 2011; Revised 22 March 2012; Accepted 3 April 2012

1. Introduction

Associated with fast social and economic growth locally, climate changes are likely to seriously impact India. As noted by Kundzewicz *et al.* (2007), southern India is already a water-stressed region. Climate changes have already been observed over the subcontinent, where increases of 0.4–0.6 °C have occurred over the past century together with the annual mean temperature warming most pronounced during post-monsoon and winter periods (Rupa Kumar *et al.*, 2006; Bhattacharya, 2007). In terms of precipitation, Cruz *et al.* (2007) have observed for the last decades that extreme summer monsoon rains increase over northwest India and the number of rainy days decrease along the east coast. While these projections are subject to large uncertainties (Paeth *et al.*, 2008), the potential impacts on water resources in India still need to be assessed depending on their location.

Global climate models (GCMs) are nowadays the only tool at disposal to investigate future climate variability. However, GCM projections cannot be used directly for impact studies due to the coarse resolution of GCM outputs which are not suited for regional assessments (Wilby *et al.*, 2004). Therefore, downscaling methods have been developed to go from large-scale data to local-scale data. The dynamical approach consists of using regional

climate models (RCMs) to resolve physical equations of atmospheric regional dynamics (Wood *et al.*, 2002). RCMs are, however, domain dependant and computationally expensive, which restricts their use for many applications. The statistical approach, on the other hand, relies on statistical relationships between large-scale GCM fields and local-scale climatic variables (such as precipitation, temperature, for instance). Statistical downscaling methods (SDMs) are quite flexible and generally require low computational costs. Such advantages make them particularly attractive for regional impact studies. SDMs can be classified into three major categories: transfer functions, weather typing and weather generators. Transfer functions are based on direct quantitative relationships between predictand and predictors through regression-like methods (Prudhomme *et al.*, 2002). Weather typing approaches consist in the grouping (or clustering) of atmospheric circulations in relation to local meteorological variables (Vrac *et al.*, 2007), while weather generators are stochastic models simulating local-scale variables based on their probability density function, whose parameters depend on large-scale information (Hughes *et al.*, 1999; Wilks and Wilby, 1999; Vrac and Naveau, 2007). Worthnotingly, a common assumption to all SDMs is that the physical relationships underlying the statistical relationships identified over a historical period remain valid for the future climate scenarios to be downscaled.

Several SDMs have already been used for downscaled rainfall over India, such as relevance (Ghosh

* Correspondence to: N. Vigaud, Service EAU, Bureau de Recherches Géologiques et Minières (BRGM), Montpellier, France.
E-mail: nicolas.vigaud@gmail.com

SDMs can also be used to model relationships between large-scale and local-scale statistical characteristics and can be referred in this context as probabilistic downscaling methods (PDMs). The cumulative distribution function transform (CDF-t) presented in Michelangeli *et al.* (2009) has the advantage of directly dealing with and providing CDFs. This method is used in this paper to downscale GCM projections from the Intergovernmental Panel on Climate Change Fourth Assessment Report (IPCC AR4) in order to investigate projected changes in both rainfall and surface temperatures over southern India. The purpose of this study is to document the use of CDF-t for providing regional precipitation and surface temperature changes as derived from several medium-term GCM projections under the Special Report on Emission Scenarios (SRES published by the IPCC) A2 scenario (horizons 2040–2060). Most of the recent statistical downscaling studies of future climate scenarios over India were restrained to the monsoon season (Tripathi *et al.*, 2006; Mujumdar and Ghosh, 2008) or to specific watersheds (Ghosh and Mujumdar, 2007; Anandhi *et al.*, 2008, 2009). This paper aims to present results from the CDF-t probabilistic downscaling method applied not only to the June–September (JJAS) monsoon period alone but to the full annual cycle, and for a domain covering the whole of southern India. In the next section, the data used and the downscaling method are presented. Then, the CDF-t approach is validated on a historical period in Section 3, prior to applying the method to downscale future scenarios from IPCC AR4 experiments in Section

seven GCMs as most reliable regarding Indian rainfall based on their representation of the monsoonal cycle in phase and amplitude. Regarding the availability of daily standard outputs from the Program for Climate Model Diagnosis and Intercomparison (PCMDI) database, five GCMs have been retained (see Table I). However, at the time of this study MIROC3.2 (medres) surface temperatures for the SRES A2 scenario were not available from the PCMDI archives. Consequently, only four GCMs will be used for the downscaling of surface temperatures. Except for CGCM3, which incorporates heat and water fluxes adjustments, the generation GCMs do not use surface flux corrections to maintain a stable climate in their control runs. Further details about the model components can be found at <http://www.pcmdi.llnl.gov/ipcc/model-documentation/>.

For the purpose of this study, simulated daily rainfall and surface temperatures have been considered from historical experiments (run 20cm³ for the 1979–1999 period) and future projections under the greenhouse gas emission scenario A2 (run A2 for the 2040–2060 period). The A2 storyline, based on high population growth, regionally oriented economic growth with significant regional disparities, widespread decline in fertility (Nakicenovic *et al.*, 2000) actually describes a very homogeneous world with less economic and technical changes than other scenarios.

Local-scale observations from the Indian Meteorological Department (IMD) are also used in this study. Daily rainfall is available from 1971 to 2005 on a 2.5-degree grid and surface temperatures from 1969 to 2005 on a 2.5-degree grid.

Table I. Climate models and their references participating in the IPCC AR4 experiments (adapted from Kripalani *et al.*, 2007). Abbreviated acronyms are used in the text to identify each GCM.

No.	Originating group	Country	IPCC ID	Abbreviation	Reference
1	Canadian centre for climate modelling	Canada	CGCM3.1 (t47)	CGCM3	Flato <i>et al.</i> (2006)
2	Météo-France/Centre National de Recherches Météorologiques	France	CNRM-CM3	CNRM3	Salas-Meade <i>et al.</i> (2006)
3	Max Planck Institute for Meteorology	Germany	ECHAM5/MPI-OM	ECHAM5	Jungelaus <i>et al.</i> (2006)
4	Bjerknes Centre for Climate Research	Norway	BCCR-BCM2.0	BCCR2	Furevik <i>et al.</i> (2003)
5	Centre for Climate System Research (The University of Tokyo) National Institute for Environmental Studies and Frontier Research Centre for Global Change (JAMSTEC)	Japan	MIROC3.2 (medres)	MIROCMR	K-1 Model Developer

The downscaling approach chosen here is the CDF-t (Michelangeli *et al.* (2009)) which can be seen as an extension of the quantile-matching method. CDF-t offers the advantage to directly deal with and provide CDFs. In its non-parametric form it does not make any assumption on the shape or family of distribution and thus can be applied separately to both rainfall and surface temperatures in the context of this study. CDF-t has already been successfully used to downscale GCMs and reanalyse 10 m wind over France by Michelangeli *et al.* (2009).

Let F_h stand for the CDF of observed local data at a given weather station (or IMD grid cell) over a historical time period h , G_h the CDF of GCM outputs bi-linearly interpolated at the station location for the same period, F_f and G_f their equivalent for the future period considered. The method is based on the assumption that there exists a transformation T translating the CDF of a GCM variable (predictor) into the CDF representing the local-scale climate variable (predictand) at the given weather station, through the transformation $T: [0, 1] \rightarrow [0, 1]$

$$T(G_h(x)) = F_h(x) \quad (1)$$

Replacing x by $G_h^{-1}(u)$ in Equation (1) with $u \in [0, 1]$ allows the following definition for the transform T :

$$T(u) = F_h(G_h^{-1}(u)) \quad (2)$$

Assuming that this later relationship remains valid in the future (i.e. $F_f = T(G_f)$), the researched CDF is given by:

$$F_f(x) = F_h(G_h^{-1}(G_f(x))) \quad (3)$$

Following Michelangeli *et al.* (2009), the CDF-t is then defined in two steps. First, estimates of (F_h, G_h^{-1}, G_f) are non-parametrically modelled. Then, their combination using Equation (3) provides an estimate of F_f . Unlike the classical quantile-matching approach which projects the simulated future large-scale values on the historical CDF to compute and match quantiles, CDF-t takes into account the change in the large-scale CDF from the historical to the future period. To downscale rainfall/surface temperatures over the full annual cycle, CDF-t is applied at each grid point to multiannual chronicles consisting of daily rainfall/surface temperatures for each month of the calendar year (all January months, February months, etc.). The resulting local-scale daily chronicles of each month

are evaluated regarding local observations from 1986–1999 for which downscaled CDFs are evaluated against IMD data using Kolmogorov–Smirnov (KS) statistics providing an estimate of the maximum difference between downscaled and observed local CDFs (Darling, 1957). The results for both rainfall and surface temperatures over southern India are presented. However, because rainfall has a discontinuity in zero, KS statistics have also been computed after removal of days with no precipitation, this analysis is further discussed in Section 3.1. In addition, dedicated diagnostics are performed for three watersheds ranging from arid (Pandam) to semi-arid (Kudaliar) to wetter conditions (South Gu). These locations are chosen to illustrate and discuss the performance of the method for different climate environments.

3.1. Precipitation regimes

Figure 1 presents KS statistics between CDFs of original GCMs rainfall (bi-linearly interpolated on a 0.5° IMD grid) as well as from downscaled GCM rainfall and IMD observed precipitation for 1986–1999. The calibration of the CDF-t over the 1971–1985 period. As mentioned previously, this KS test is performed at each grid point; therefore, the box-plots displayed in Figure 1 represent the spatial dispersion of the KS statistics for the whole of the South India domain. For the different periods, the different GCMs downscaled rainfall are characterized by a spatial dispersion comparable to the original GCM outputs. For the full year (top panel) and for all GCMs, even if they stay above the threshold of statistical significance (0.019 at 0.05 significance level, not plotted), KS scores are substantially improved for downscaled daily rainfall compared to raw GCM data. Similar results are found for the monsoon period. Maximum KS scores computed in Figure 1 actually occur at the discontinuity of rainfall in zero, and the results thus show that dry days are better represented in downscaled fields than in original GCM outputs compared to observation. This is consistent with the fact that dry days are generally rare in GCMs. Consequently, similar KS scores have been plotted in Figure 2 after removal of days with no rainfall (zero values) in all precipitation dataset. For the whole year, results are very contrasted depending on GCMs. CDF-t seems to perform best in the case of ECHAM5, which downscaled rainfall are closer to observation than original GCM outputs. While there is no improvement

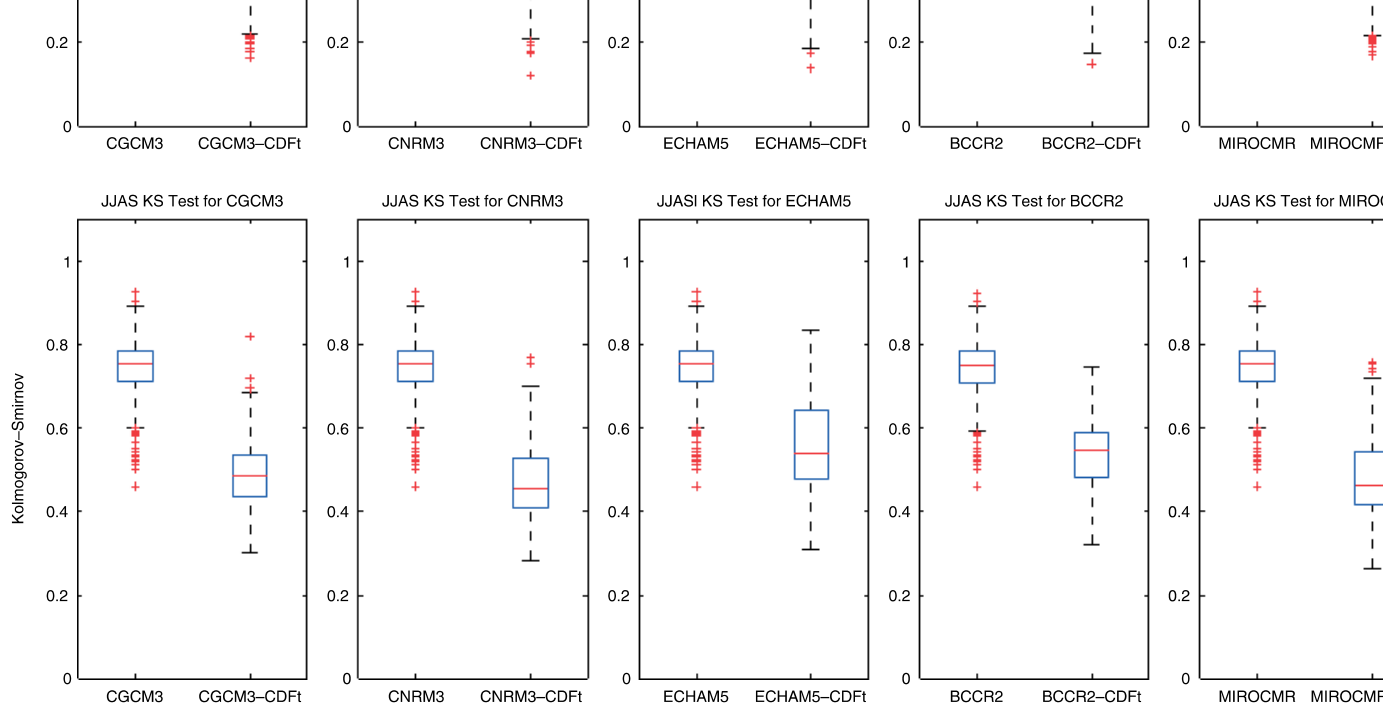


Figure 1. Kolmogorov–Smirnov statistics for original (left box-plots) and downscaled (right box-plots) GCMs rainfall when compared to observation data over the 1986–1999 period for the whole of southern India, with calibration of the CDF-t over 1971–1985. Statistics for the full year and the JJAS period are presented in the top and bottom panels, respectively.

for CNRM3, the performance of the method is mitigated in the case of BCCR2, MIROC MR and CGCM3. For the JJAS period however, downscaled rainfall using CDF-t are all closer to observation than original GCMs data, witnessing of a good performance of CDF-t over the monsoon season.

In addition, downscaled GCMs daily rainfall fields are evaluated in regards to the seasonal cycle and mean monsoon precipitation rate over the validation period 1986–1999. Mean rainfall seasonal cycles shown in Figure 3 for Pandam Eru, Kudaliar and South Gundal locations (referenced in Figure 4) suggest for all GCMs, substantial improvements for downscaled data compared to large-scale outputs. The gain appears to be better for humid (South Gundal) and semi-arid (Kudaliar) regions than for arid areas (Pandam Eru), illustrating the varying performance of the method depending on climatic environments.

The mean JJAS pattern from IMD observed rainfall (Figure 4 upper right panel) shows maximum rainfall rates over the northeastern regions and along the west coast, while minimum values over central southern India separate these two regions. Clearly, such a structure is not found accurately in any of the GCMs used in this study. Nevertheless, these gradients are well reproduced in downscaled rainfall fields for all GCMs. The main

differences between downscaled GCMs data are characterized by the amplitudes of the above extremes over the monsoon season: for instance, greatest maximum values over northeast India are found for CNRM3, downscaled rainfall while central regions of southern India are the least dry for BCCR2 resulting local-scale data.

Dry spells lengths PDFs at Pandam Eru, Kudaliar and South Gundal locations are shown for original and downscaled GCMs together with IMD observation in Figure 5. The different climatic conditions over these watersheds are well represented from observed rainfall with increasing slopes from arid to wetter climate. Inflexions within short dry spells lengths suggest that most dry spells have a duration below five days but with varying proportion over all watersheds, short dry spells being less prevalent for arid and semi-arid regions (60–70%) than for wetter climate (almost 80%). These differences are less clear for the original GCMs (dashed coloured lines): large biases are found concerning both slopes and proportion of short and long spells. Nevertheless, downscaled fields (thick coloured lines) systematically exhibit a better representation of dry spells lengths compared to raw GCMs rainfall. In arid (Pandam Eru) and semi-arid (Kudaliar) regions, among these locations out of the five GCMs dataset, ECHAM5 appears to be the closest to observed dry spells

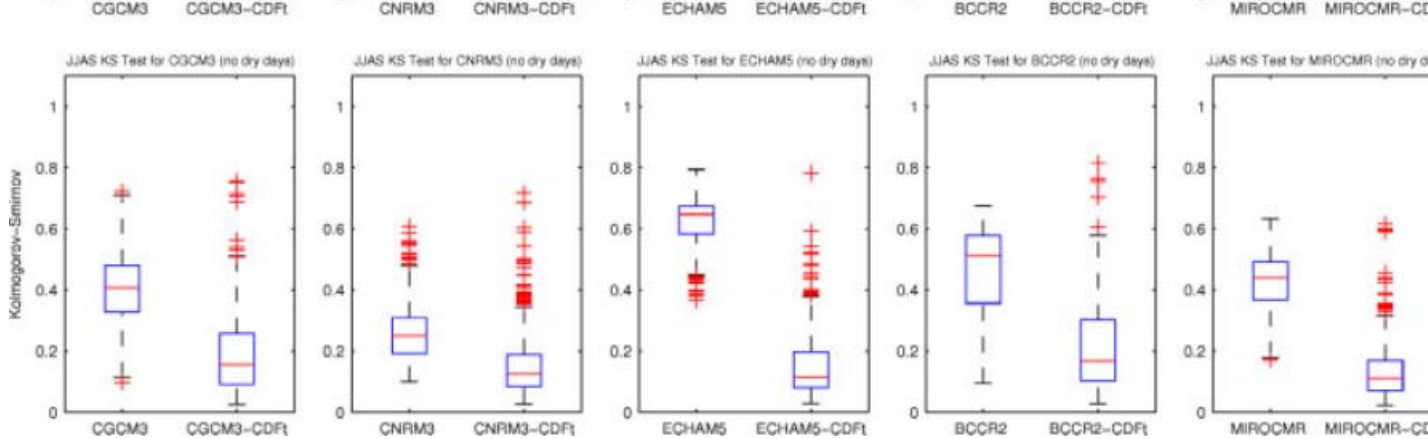


Figure 2. Similar to Figure 1 but after removal of days with no rainfall.

from IMD data, similarly for downscaled fields, down-scaled ECHAM5 rainfall provide the best results. The remaining four GCMs display larger biases while substantial gains in dry spells representation characterize their corresponding downscaled rainfall fields. For wetter climatic conditions (South Gundal), similar but less efficient improvements are noticeable between original and downscaled GCMs precipitation except in the case of ECHAM5 for which dry spells lengths PDF from original GCM outputs seems closer to IMD observation than the resulting downscaled data. This could indicate a lesser performance of the CDF-t method for wetter climatic regions in terms of dry spells lengths.

Finally, JJAS anomalies over the 1986–1999 period for original and downscaled GCMs rainfall at the different watersheds (not shown) suggest that interannual variability within the resulting local-scale data is driven by the GCM outputs. Compared to IMD observations, no GCM seems able to reproduce the observed year to year monsoon rainfall variability, and such is the case regarding their corresponding downscaled fields.

3.2. Surface temperatures

Regarding annual fields, even though some scores are still above significance level (not plotted), KS statistics shown in Figure 6 (top panels) exhibit systematic improvements for downscaled GCMs surface temperatures when compared to observation. Interestingly, the spatial dispersion of the KS is much smaller for the resulting high resolution fields than for original GCMs data. Concerning the monsoon period, no such gain is found for JJAS KS diagnostics (Figure 6 bottom panels): except from CNRM3, statistical scores are similar to those obtained for original GCMs data.

Mean surface temperatures seasonal cycle at Pa Eru, Kudaliar and South Gundal locations are presented in Figure 7 for the 1986–1999 period. For all watersheds, in dry or more humid conditions, downscaled fields systematically improved compared to original GCM surface temperatures and are fitting closely the observations over this historical period.

All mean JJAS GCMs downscaled surface temperatures (Figure 8) display patterns close to what is observed for IMD data while fields from original GCMs presenting substantial biases. In particular, the latitudinal gradient along the west coast which is subject to marked discrepancies in large-scale GCM outputs, is represented in all downscaled data. The meridional gradient from western to eastern parts of the subcontinent is also better reproduced in resulting local-scale surface temperatures, with a more or less marked minimum in northeastern regions, as found in IMD observation.

Mean JJAS surface temperatures differences between the validation (1986–1999) and calibration (1971–1999) periods are plotted in Figure 9 for raw GCM outputs and IMD observations. Noteworthy, no much difference is found for IMD observations but also for CNRM3, while other GCMs are characterized by more or less marked variations. Given that CDF-t downscaled fields are strongly driven by the evolution of the original GCM outputs, this could explain the poor JJAS KS scores in Figure 6 for CGCM3, ECHAM5, and BCCR2 results for local-scale data.

In addition, JJAS surface temperature anomalies at different watersheds locations for the 1986–1999 period (not shown) exhibit substantial discrepancies in terms of interannual variability for raw GCM outputs when compared to observations. Here again, these differences remain in the downscaled data.

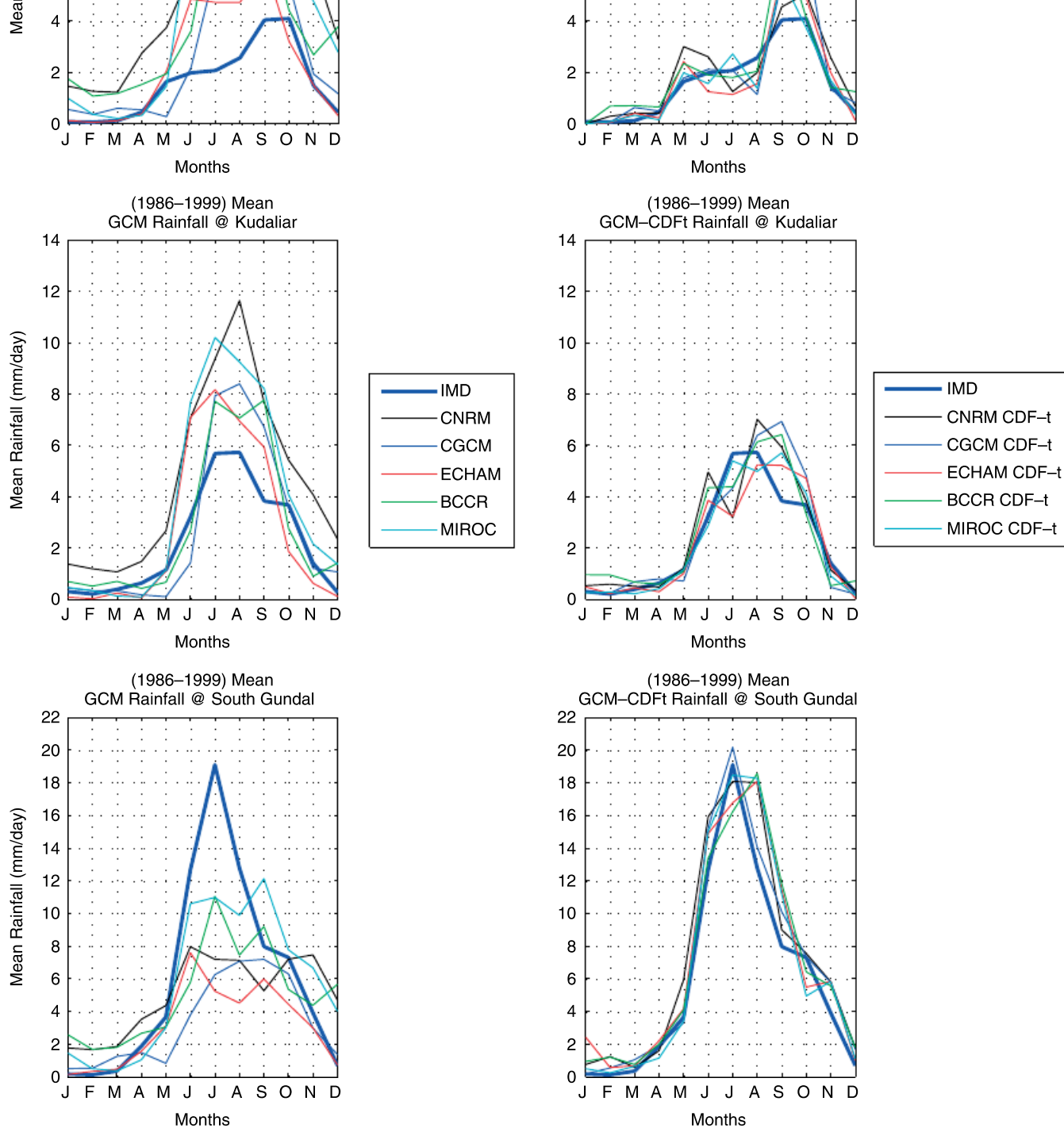


Figure 3. Mean seasonal cycle (in mm d^{-1}) at Pandam Eru (top panel), Kudaliar (middle panel) and South Gundal (bottom panel) location. Left column shows original (left) and downscaled (right) GCMs rainfall together with IMD observation (thick blue line) over the 1986–1999 period, with calibration of the CDF-t over 1971–1985.

4. Application to projected GCM A2 scenarios

The CDF-t method is now applied to downscale large-scale precipitation and surface temperature projections from IPCC AR4 experiments under the greenhouse gas emission scenario A2 over southern India. As for the historical period, resulting high resolution fields

are generated by applying CDF-t by months on the GCM outputs. Regarding the availability of daily rainfall data for the GCMs selected within the PCMDI project, the period 2046–2065 (hereafter A2 period) is the period used for downscaling future A2 scenarios at medium resolution. The 1971–1999 period is used for calibration of the CDF-t in order to take advantage of the longest period

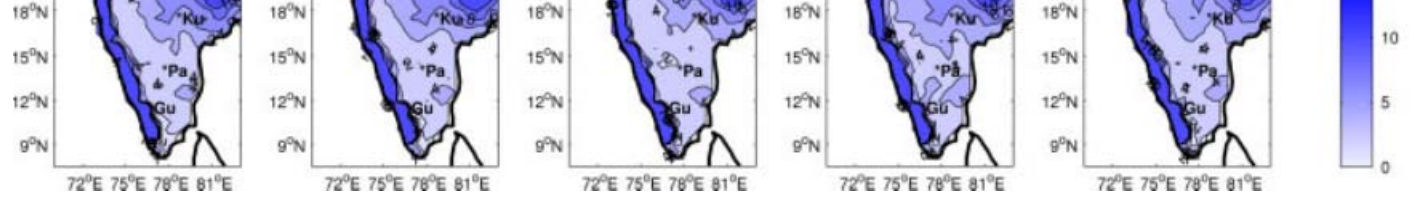


Figure 4. Mean June to September rainfall (in mm d^{-1}) for original (top panels) and downscaled (bottom panels) GCMs data together with observation (top right) over the 1986–1999 period for the whole of southern India, with calibration of the CDF-t over 1971–1985. Pandam Eru (Pa), Kudaliar (Ku) and South Gundal (Gu) locations are referenced on the maps for indication.

observation available from IMD. It is worth noting that the aim of this paper is not to fully investigate the potential impacts of climate change over southern India but rather to document the use of the CDF-t method for statistical downscaling of a future climatic scenario over the full year cycle.

4.1. Projected rainfall changes

Projected large-scale as well as downscaled GCM outputs are now compared to their corresponding 1971–1999 fields using KS tests (Figure 10). For both the annual cycle and the monsoon period, systematic higher KS scores, are found for downscaled data. In the light of Section 3.1 the medians (red lines) would indicate more dry days for A2 scenario projections than for the contemporary period. When computing KS after removal of days with no rainfall (zero values) very similar plots were obtained (not shown), suggesting more pronounced projected climate changes in local-scale precipitation than for raw GCM outputs. The results obtained also exhibit a greater spatial dispersion for downscaled fields relatively to original large-scale GCM outputs, suggesting that resulting changes linked to climate change are more contrasted geographically at local-scale for all GCMs.

Mean seasonal rainfall changes are shown in Figure 11 at Pandam Eru (left), Kudaliar (centre) and South Gundal (right) locations for all downscaled GCMs individually. In order to have a benchmark to which CDF-t downscaled fields could be compared, the differences of GCMs seasonal cycles between two 20 year periods have been computed to represent the climate change signal as depicted in the raw GCMs data. Hereafter, rainfall changes are calculated relative to the historical 1980–1999 period (XX period in the following).

The dispersion within the different GCMs projected changes illustrates clearly the need to consider a panel of GCMs for climate change impact studies over southern India. In terms of mean GCMs ensemble, the CDF-t method gives similar results to original GCM outputs:

most pronounced changes are found during the monsoon season over all watersheds with maximum variations during May–June and August. Nevertheless, as in the case from JJAS KS scores discussed previously, changes in precipitation between the A2 and XX periods seem to differ in magnitude from one location to another. For the arid Pandam Eru basin, maximum changes are just below 1 mm d^{-1} in June and August (representing approximately a 15% increase of the monthly mean precipitated amount) with very small differences between CDF-t results and original GCM fields. At Kudaliar raw GCMs data exhibit similar changes (below 1 mm d^{-1}) while the CDF-t method shows variations of about 2 mm d^{-1} (about 50% increase) in June. For the wetter South Gundal location, differences increase between CDF-t downscaled fields and original GCM outputs. Maximum downscaled precipitation changes are rather from about 1 mm d^{-1} (1.5 mm d^{-1} for raw GCM outputs) in May–June to 1.5 mm d^{-1} (2.8 mm d^{-1} for original GCMs data) in August (about 10% to 15% increase). While differences in CDF-t projected and GCMs original rainfall changes seem to increase from arid to wetter climatic regions of southern India, noteworthingly the dispersion within downscaled GCMs climate change signals also becomes more pronounced. In addition, weak positive changes are found during the dry season, most particularly from October to April, from the CDF-t method as well as from raw GCMs data. At Pandam Eru location, both the CDF-t approach and original GCMs rainfall exhibit variations just below zero from October to December while no substantial changes seem to appear from January to April. Similar results are found for raw GCM outputs at Kudaliar while negative changes are slightly more pronounced for CDF-t estimates (about 0.5 mm d^{-1} corresponding to a 50% decrease). For more substantial negative changes are characteristic of the South Gundal basin: the CDF-t approach and original GCMs data suggest most pronounced rainfall decreases from October/November to December (up to 1 mm d^{-1}).

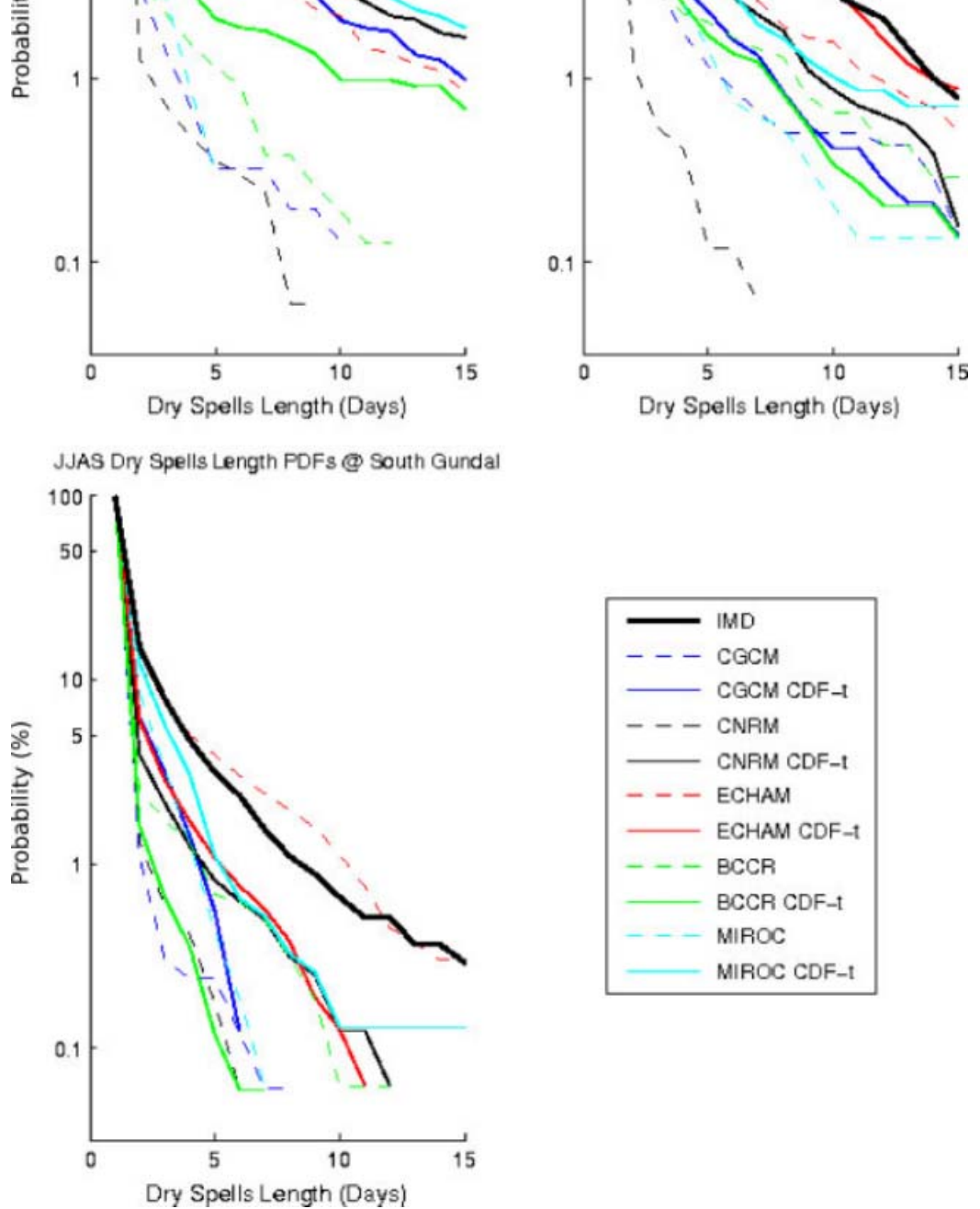


Figure 5. Dry spells length PDFs (in %) at Pandam Eru (top left), Kudaliar (top right) and South Gundal (bottom) locations for original (thin coloured lines) and downscaled (thick coloured lines) GCMs data together with IMD observations (black thick line) over the 1986–1999 period. The thick lines are obtained with calibration of the CDF-t over 1971–1985.

about 80% of precipitated amounts) respectively while negative variations from January to April are less substantial (maximum about 0.5 mm d^{-1} in March, about 50% decrease). Overall, these results corroborate findings from previous studies emphasizing enhanced precipitation over southern India, mostly during the monsoon season (Rupa Kumar *et al.*, 2006; Tripathi *et al.*, 2006; Kripalani *et al.*, 2007; Anandhi *et al.*, 2008).

Regarding JJAS rainfall means (Figure 12 two top panels), downscaled fields are more coherent with the known

climatology from IMD data for the historical period (Figure 4) than raw GCMs. In particular, maximum precipitated amounts along the west coast and northern regions of the subcontinent as well as the central patterns associated to more arid regions, are well represented in the resulting downscaled fields from all GCMs. Of course, there is no benchmark to compare future projections, nevertheless these regional variations appear more realistic for downscaled rainfall than for the original GCM projections. Moreover, the spatial changes

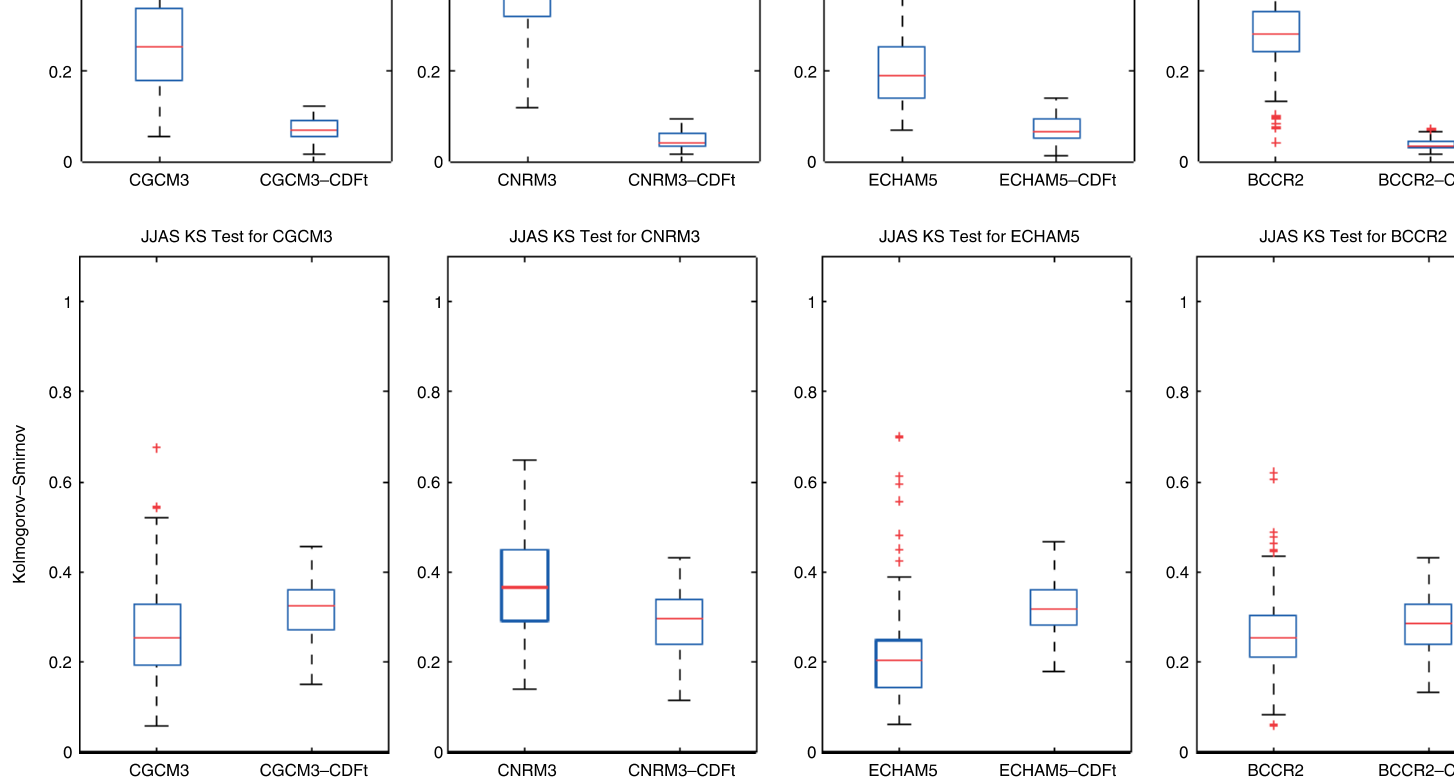


Figure 6. Kolmogorov–Smirnov statistics for original (left box-plots) and downscaled (right box-plots) GCMs surface temperature compared to IMD observation data over the 1986–1999 period for the whole of southern India, with calibration of the CDF-t over 1971–2000. Statistical scores for the full year and the JJAS period are presented in the top and bottom panels, respectively.

JJAS rainfall obtained for individual GCM downscaled data (Figure 12 bottom panels) are systematically comparable to these from their corresponding raw GCM outputs. The amplitudes of these variations however appear to be enhanced for the resulting high resolution fields, corroborating findings from JJAS KS scores (Figure 10), with most pronounced differences over western coastal areas and northeastern regions of the subcontinent.

Differences in dry spells lengths PDFs between the A2 and XX periods are presented for the three watersheds in Figure 13. At all locations, maximum changes are found for short dry spells lengths (below 5 d) with enhanced variations for the downscaled fields when compared to raw GCM outputs. At Pandam Eru and Kudaliar, the mean GCM A2 projections in JJAS are characterized by a reduction of very short dry spells (below 2 d), while dry spells with a duration above 2 d are likely to increase. The reverse is found for the wetter South Gundal basin with enhanced very short dry spells occurrences and a reduction of longer periods without rain (above two days) during the monsoon season. Interestingly similar results are found from mean raw GCM projections at Kudaliar and South Gundal locations with some differences in terms of magnitude of these changes. However, original

GCMs data would rather suggest a slight increase in very short dry spells at Pandam Eru contrasting with the reduction suggested by the resulting high resolution

4.2. Projected surface temperatures

Surface temperature variations associated with rainfall regime changes are examined here in order to provide a further description of A2 scenario projections consistent with the findings in this study. As mentioned in Section 2.1, due to the unavailability of daily surface temperatures data for the 2046–2065 period, only four GCMs will be used in this part (MIROC MR daily surface temperatures are unavailable from PCMDI archives at the time of this study).

Similarly to Figure 10, KS diagnostics characterize the surface temperatures evolution for both the full annual cycle and the monsoon season for all GCMs (Figure 11). As shown by their respective median, a signal with a similar amplitude is recovered from the original and downscaled GCMs data between the contemporary period and the projected A2 scenario, downscaled median values being a little lower than for raw GCMs except for ECHAM5. A slightly higher spatial dispersion is observed for CGCM3, ECHAM5 and BCCR2 downscaled

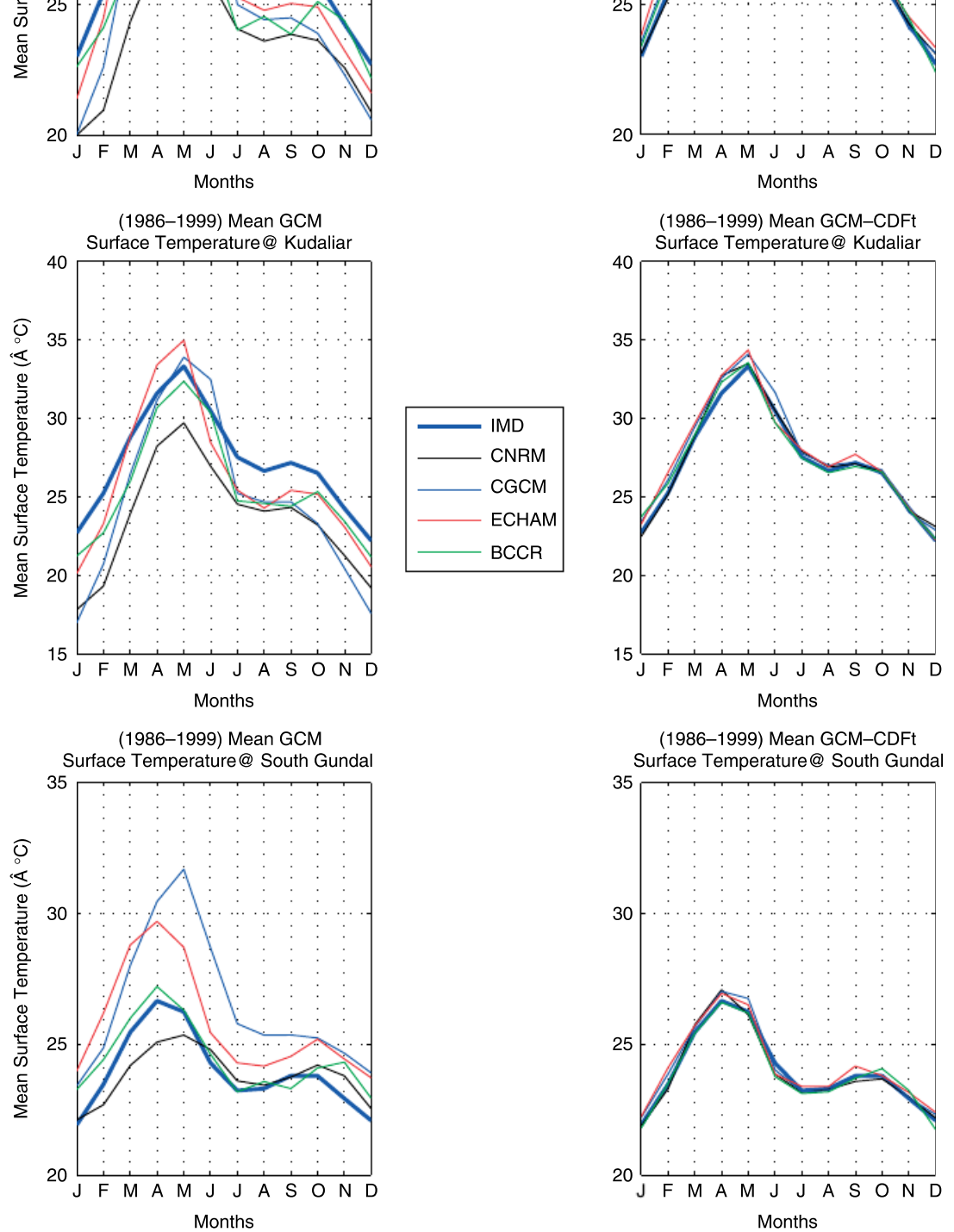


Figure 7. Mean seasonal cycle (in °C) at Pandam Eru (top panels), Kudaliar (middle panels) and South Gundal (bottom panels) location. Left panels show original (left) and downscaled (right) GCMs surface temperatures together with IMD observation (thick blue line) over the 1986–1999 period. Right panels show downscaled GCMs surface temperatures with calibration of the CDF-t over 1971–1985.

compared to GCM outputs, but overall the KS scores are roughly of the same order for both the full year and the monsoon season. Such results would suggest very similar evolutions between the A2 and XX periods for large-scale GCMs and downscaled surface temperatures.

Mean surface temperatures seasonal differences from the XX to the A2 periods with the CDF-t method are

compared in Figure 15 with raw GCMs. Both downscaled fields and raw GCMs data lead to similar conclusions in terms of GCMs ensemble mean surface temperature. Despite the dispersion within all GCMs realizations, GCMs ensemble mean surface temperature appear to be more pronounced over arid and semi-arid basins (Pandam Eru and Kudaliar respective

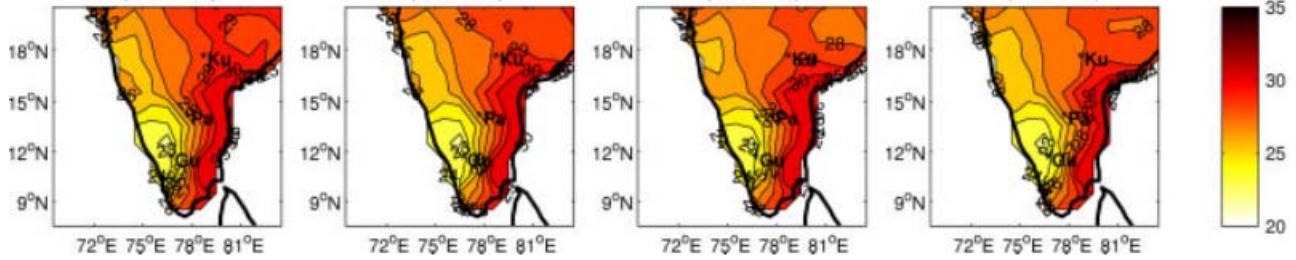


Figure 8. Mean June to September surface temperatures (in °C) for original (top panels) and downscaled (bottom panels) GCMs data compared with IMD observation (top right) over the 1986–1999 period for the whole of southern India, with calibration of the CDF-t over 1971–1985.

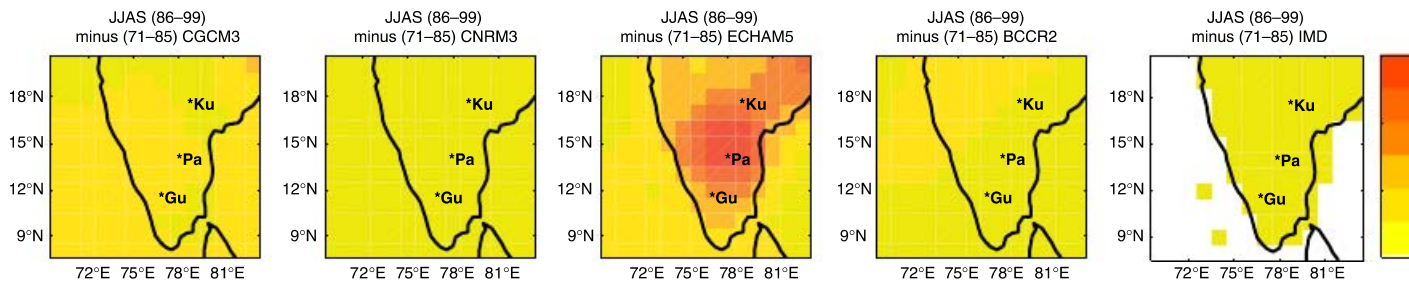


Figure 9. Mean JJAS surface temperatures differences (in °C) between the validation (1986–1999) and calibration (1971–1985) periods for the whole of southern India for the GCMs and IMD observations.

for wetter environment (South Gundal). Nevertheless, maximum surface temperature changes for all watersheds are found during the dry season, most particularly in February–March (about 2.5°C at Pandam Eru and Kudaliar, and 2.2°C at South Gundal). Smaller variations are found during the monsoon season with minimum changes in August (about 1.5°C for all watersheds). These findings are in agreement with other studies emphasizing an increasing trend in mean annual surface temperatures with a more pronounced warming during the post-monsoon and winter seasons (Bhattacharya, 2007). Moreover, it appears that arid and semi-arid areas are where the seasonal amplitude of surface temperatures projected changes would be maximum.

In Figure 16 are shown mean JJAS surface temperatures for original/downscaled (top panels/2nd line from top) GCM outputs under the A2 scenario (2046–2065) and their respective differences (3rd/4th lines) with original/downscaled GCMs data for the historical period (1980–1999). Again, there is no reference to which downscaled fields can be compared to for the projected scenario. Nevertheless, in regards to the mean JJAS climatology from IMD observations over the contemporary period (see Figure 8), the patterns found in all GCMs downscaled data is far more coherent than raw GCMs surface temperatures, in particular regarding the

latitudinal gradient along the west coast and the regional gradient inland. Concerning surface temperature changes between the A2 and XX periods, similar patterns characterize both original and downscaled data. The amplitude of these projected changes are comparable between large-scale and downscaled data, except for ECHAM5 for which downscaled changes are slightly greater, agreeing with the findings from Figure 16 discussed previously. ECHAM5 projections depict more pronounced changes (up to 3°C) over northern regions of the subcontinent while the other GCMs suggest minimum surface temperature increases (from 1 to 2°C) in southern regions. Interestingly, for CGCM3 and BCCR2 regions of maximum surface temperatures changes in JJAS correspond approximately to areas of maximum monsoon rainfall increases. Recent studies have emphasized, from multi-model projections, the intensification of different pressure systems at play over the region and enhanced moisture advection from the oceans (Kripalani *et al.*, 2007). This could suggest a possible increase of local convection in these two GCMs projections. However, the possible linkages between monsoon fall and surface temperatures changes for CNRM3 and ECHAM5 are less clear from the short diagnostics presented in this paper and deeper research is needed in order to give further elements of description relative to the processes at play.

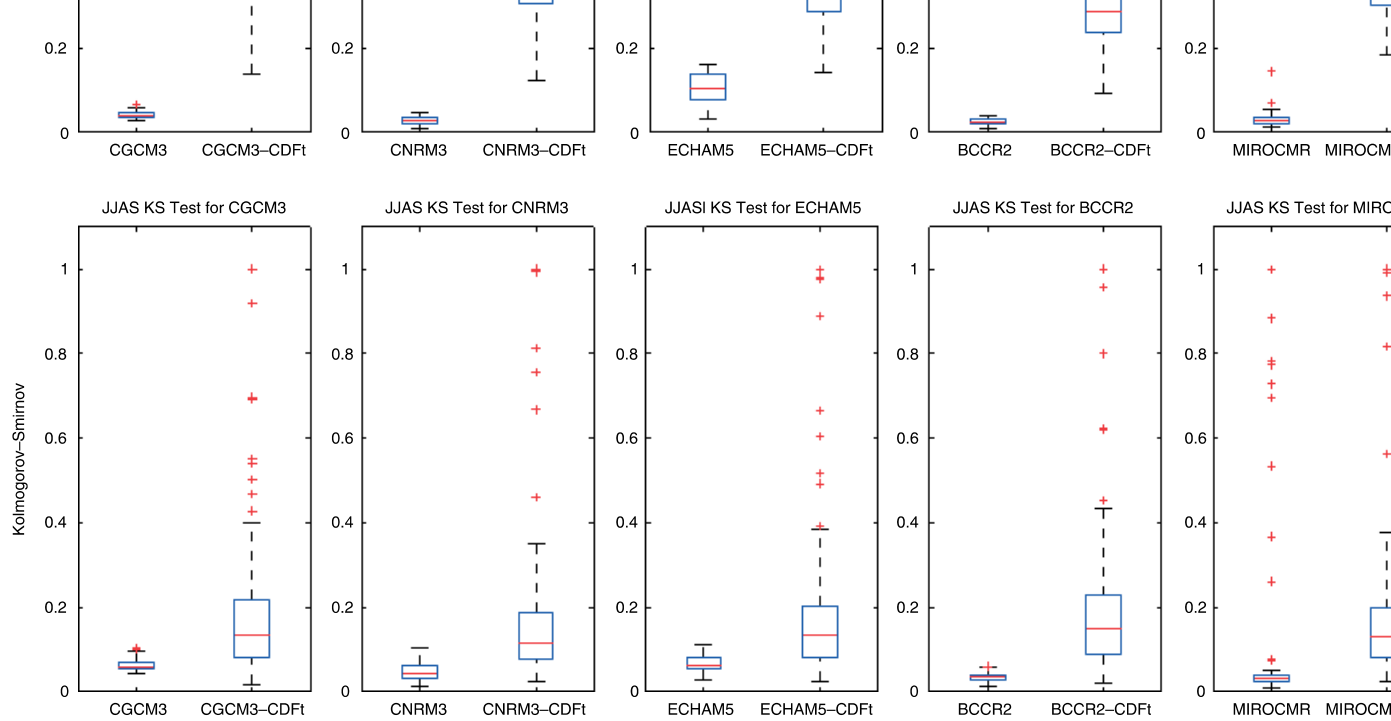


Figure 10. Kolmogorov–Smirnov statistics between original (left box-plots) and downscaled (right box-plots) GCMs rainfall for the A2 scenario (2046–2065) and the 1971–1999 calibration period for the whole of southern India. Scores for the full year and the JJAS period are shown in the top and bottom panels, respectively.

5. Discussion and conclusions

In order to downscale GCM projections over southern India for the whole annual cycle, the CDF-t method (Michelangeli *et al.*, 2009) has been applied to monthly chronicles of daily large-scale rainfall and surface temperatures. First, CDF-t has been validated on the 1986–1999 period and compared to historical IMD observations. In terms of KS statistics, resulting local-scale fields exhibit substantial improvements in comparison to original GCM outputs regarding distribution characteristics but also mean seasonal cycle and monsoon means for both precipitation and surface temperatures. Then, the CDF-t method has been applied to GCMs climate simulations of the 21st century under the SRES A2 scenario. Resulting high resolution fields have been compared to original GCM outputs at different locations (arid, semi-arid and wetter environment) where both lead to similar conclusions. Concerning precipitation, the results show a substantial increase of rainfall in particular during the monsoon season and for semi-arid and wetter climatic zones (from about 15 to 50%) while winter precipitation are generally reduced (maximum decrease of about 50–80% for wetter climatic regions) in accordance with previous findings (Rupa Kumar *et al.*, 2006; Kripalani *et al.*, 2007; Raje and Mujumdar, 2009). These changes

are accompanied by increases in surface temperature, most pronounced during the post-monsoon (up to 2°C) and winter season at all locations also agreeing with earlier studies (Rupa Kumar *et al.*, 2006; Bhattarai, 2007).

This method was used to provide local-scale estimates of variables for impact studies (hydrological and agricultural and economical) at basin scale over southern India, a stressed region where the impacts of global change are expected to increase significantly (Kundzewicz *et al.*, 2009). Most statistical downscaling studies generally focus on a single season (for example JJAS) and downscaling projections from different GCMs for the full year are rarely documented. The monthly approach chosen here gave better results than for the full year (not only for precipitation and supports findings from other studies regarding the need to seasonalize SDMs for better projected local estimates (Tripathi *et al.*, 2006).

The same non-parametric approach was chosen for this study to downscale separately rainfall and surface temperatures. However, in the case of rainfall, the ‘occurrences’ (which are particularly important during the dry season) may need more development. Days without precipitation are generally not adequately represented in GCM outputs, and this could affect

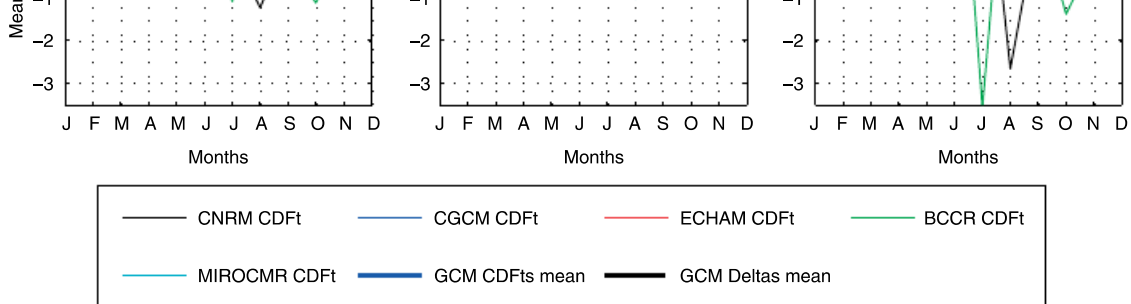


Figure 11. Mean seasonal rainfall cycle changes (in mm d^{-1}) at Pandam Eru (left panel), Kudaliar (middle panel) and South Gundal (right panel) locations between the A2 (2046–2065) and XX (1980–1999) periods seen by CDF-t compared to results from raw GCMs outputs.

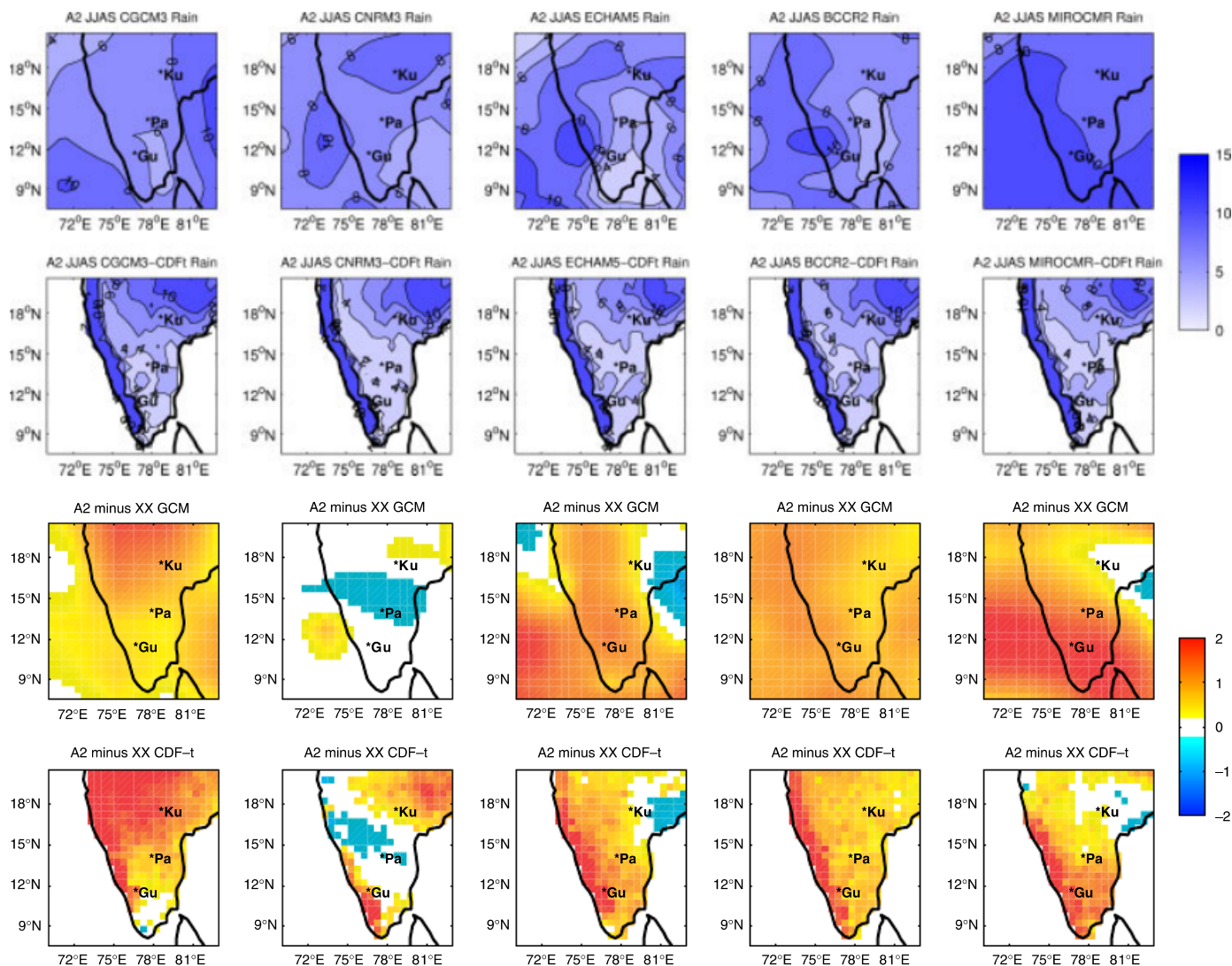


Figure 12. Mean June to September original (top panels) and downscaled (second line) GCMs rainfall for the A2 scenario (2046–2065) in southern India as well as the original GCMs (third line) and CDF-t projected (bottom panels) changes (in mm d^{-1}) when compared to historical XX period (1980–1999).

CDF-t formulation used for downscaling rainfall. As shown in Section 3.1, dry days are better represented in downscaled precipitation than in GCMs data when compared to observation. Nevertheless, for all GCMs

CDF-t seems to perform better, in terms of dry days and precipitated amount, during the monsoon season with ‘no-precipitation’ occurrences, than for the whole year. To address this issue, a next step would be to use

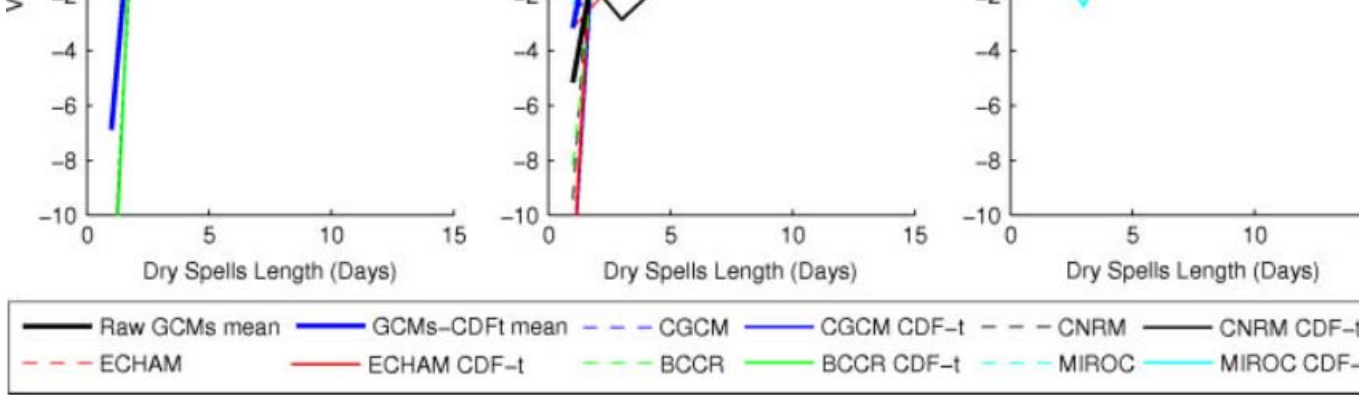


Figure 13. Differences in dry spells length PDFs (in %) at Pandam Eru (left), Kudaliar (centre) and South Gundal (right) locations for raw GCMs mean (dashed coloured lines) and downscaled (thick coloured lines) GCMs data between the A2 (2046–2065) and XX (1981–1999) 20 year periods.

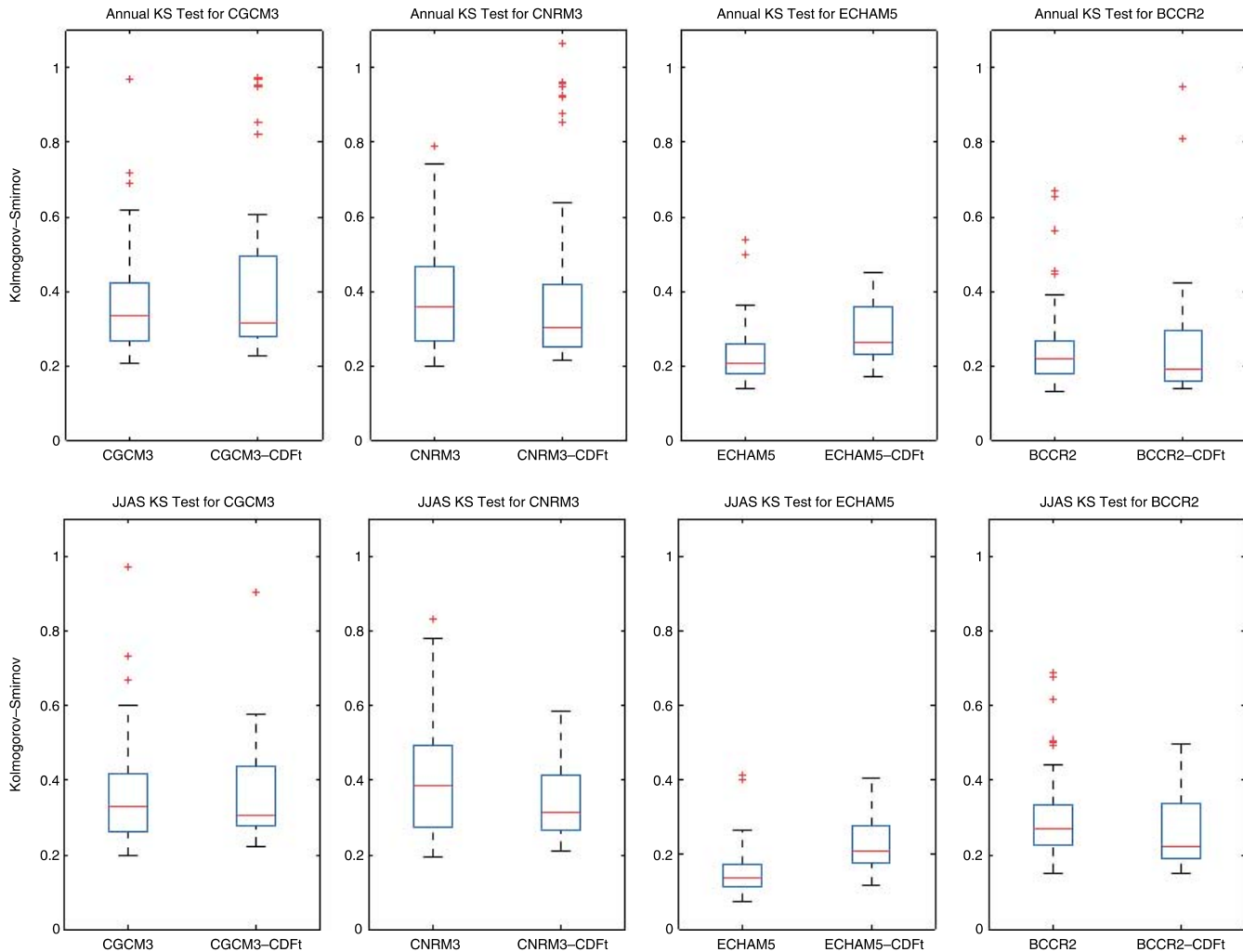


Figure 14. Same as Figure 10 but for surface temperatures.

relevant distribution models for precipitation through a parametric approach as it has been done with other SDMs using Gamma or mixed distributions for example (Vrac and Naveau, 2007).

Nevertheless, CDF-t proved to be an interesting and efficient statistical tool, offering substantial perspectives in terms of downscaling and climate change studies at local-scale, with the low computational cost.

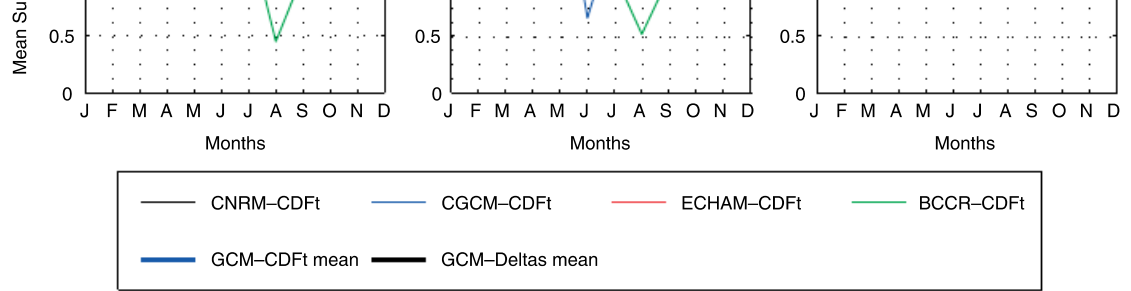


Figure 15. Same as Figure 11 but for surface temperatures (in °C).

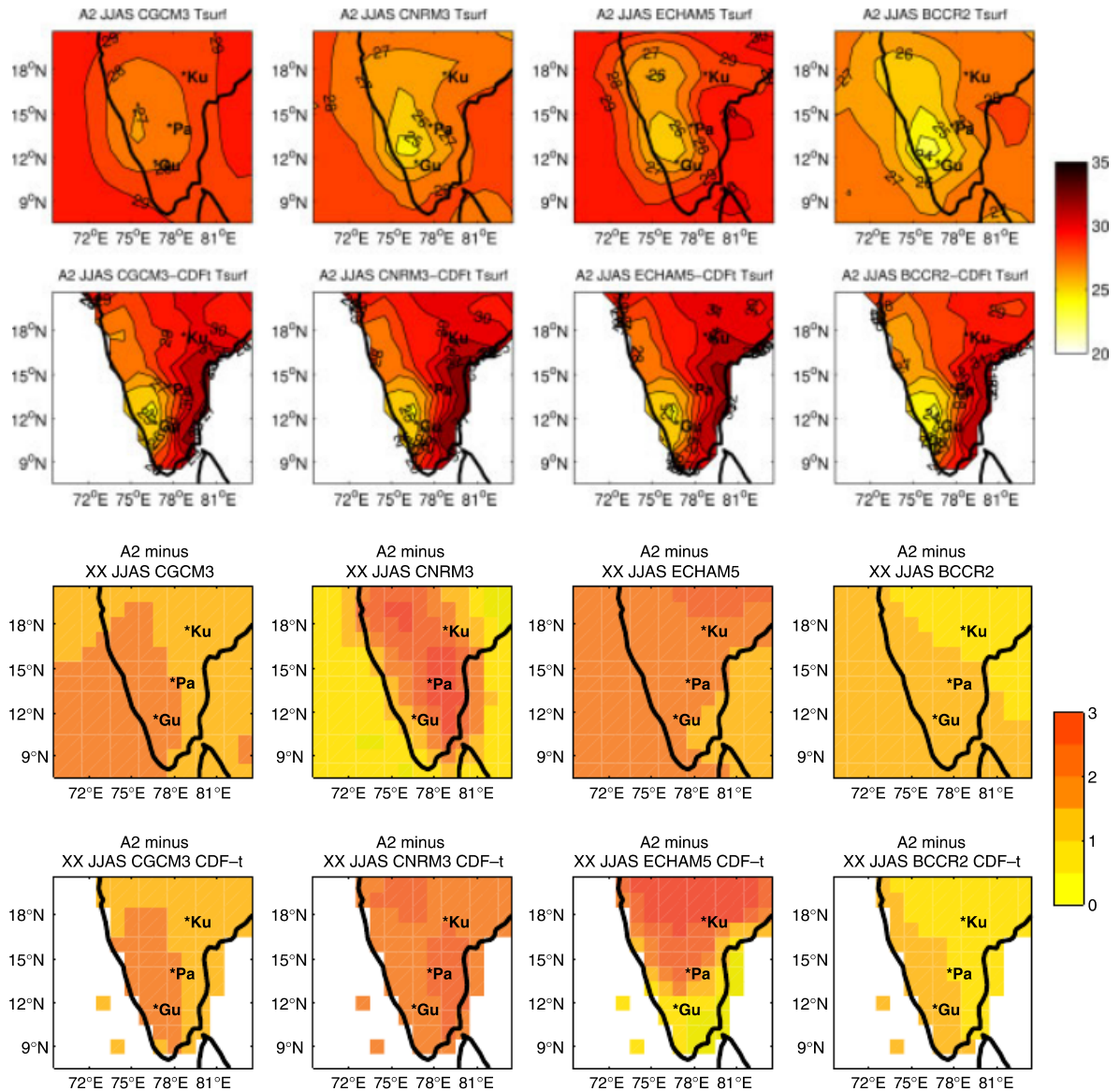


Figure 16. Same as Figure 12 but for surface temperatures (in °C).

and flexibility of this approach making it even more attractive.

Finally, deeper research is needed to give further elements of description regarding future climatic projections over southern India and the processes involved.

First the period of study regarding these projections is limited to 20 years and could be extended. It is also relevant to compare our results to projections obtained through numerous statistical downscaling approaches (other than the single delta method) in

rainfall and surface temperatures over the Indian region. However, this paper corresponds to one more step in that direction helping to document medium-range future climatic scenarios (2040–2060), these horizons being crucial for local adaptation strategies.

Acknowledgements

This study has been supported by the Agence Nationale pour la Recherche (ANR) through the VMCS program (project SHIVA contract ANR-08-VULN-010-01) and the Bureau de Recherches Géologiques et Minières (BRGM). The authors thank the SHIVA partners for their contribution. Mathieu Vrac was partially funded by the GIS-REGYNA Project. IMD observations were obtained from the Institute of Meteorology Department of India. GCM outputs from the IPCC AR4 exercise were downloaded from the PCMDI server (http://www.pcmdi.llnl.gov/ipcc/model_documentation/). The downscaling has been realized with the ‘CDF-t’ R package freely available on the CRAN website (<http://cran.r-project.org/>).

References

- Anandhi A, Srivanas V, Kumar DN, Nanjundiah RS. 2009. Role of predictors in downscaling surface temperature to river basin for IPCC SRES scenarios using support vector machine. *International Journal of Climatology* **29**: 583–603.
- Anandhi A, Srivanas V, Nanjundiah RS, Kumar DN. 2008. Downscaling precipitation to river basin in India for IPCC SRES scenarios using support vector machine. *International Journal of Climatology* **28**: 401–420.
- Bhattacharya S. 2007. Lessons learnt for vulnerability and adaptation assessment from India's first national communication, vol 7, BASIC EU Project.
- Cruz R, Harasawa M, Wu S, Anokhin Y, Punsalma B, Honda Y, Jafari M, Li C, Ninh NH. 2007. *Asia Climate Change 2007: Impacts, Adaptation and Vulnerability. Contribution of Working Group II to the Fourth Assessment*. Cambridge University Press: UK, 469–506.
- Darling D. 1957. The Kolmogorov-Smirnov, Cramer-von Mises tests. *Annals of Mathematical Statistics* **28**: 823–838.
- Flato GM, Boer GJ, Lee WG, McFarlane NA, Ramsden D, Reader MC, Weaver AJ. 2000. The Canadian Centre for Climate Modeling and Analysis of Global Coupled Model and its climate, *Climate Dynamics* **16**: 451–467.
- Furevik T, Bentsen M, Drange H, Kindem IKT, Kvamsto NG, Sorteberg A. 2003. Description and evaluation of the Bergen Climate Model: ARPEGE coupled with MICOM, *Climate Dynamics* **21**: 27–51.
- Ghosh S, Mujumdar P. 2007. Nonparametric methods for modelling GCM scenario uncertainty in drought assessment. *Water Research* **43**: W07405, 19 pp., DOI: 10.1029/2006WR005351.
- Ghosh S, Mujumdar P. 2008. Statistical downscaling of GCM

- Kundzewicz Z, Mata L, Arnell N, D'Il P, Kabat P, J Miller K, Oki T, Sen Z, Shiklomanov I. 2007. *Freshwater and their Management*. Cambridge University Press: UK.
- Michelangeli P, Vrac M, Loukos H. 2009. Probabilistic approaches: application to wind cumulative distributions. *Geophysical Research Letters* **36**: L11708, 6 pp., DOI: 10.1029/2009GL038401.
- Mujumdar P, Ghosh S. 2008. Modelling GCM and scenario uncertainties using a possibilistic approach: application to the River. *Water Resources Research* **44**: W06407, 15 pp., DOI: 10.1029/2007WR006137.
- Nakicenovic N, Davidson O, Davis G, Grbler A, Kramarski L, Metz B, Morita T, Pepper W, Pitcher H, Sankovski P, Swart R, Watson R, Dadi Z (eds). 2000. In *Special Emissions Scenarios: A Special Report of Working Group III of the Intergovernmental Panel on Climate Change*. Cambridge University Press: 599.
- Paeth H, Scholten A, Friederichs P, Hense A. 2008. Uncertainty in climate change prediction: El Nino-Southern Oscillation monsoons. *Global and Planetary Change* **60**: 265–288.
- Prudhomme C, Reynard N, Crooks S. 2002. Downscaling climate models for flood frequency analysis: where are we? *Hydrological Processes* **16**: 1137–1150.
- Raje D, Mujumdar P. 2009. A conditional field-based downscaling method for assessment of climate change impact on multi-scale precipitation in the Mahanadi basin. *Water Resources Research* **45**: W10404, 20 pp., DOI: 10.1029/2008WR007487.
- Rajeevan M, Bhat J. 2008. A high resolution gridded rainfall dataset (1971–2005) for mesoscale meteorological studies. *Journal of Earth System Science* **118**: 101–115. Research Report.
- Rupa Kumar K, Sahai A, Kumar KK, Patwardhan S, Revadekar J, Kamala K, Pant G. 2006. High-resolution climate change scenarios for India for the 21st century. *Current Science* **90**(3): 334–345.
- Salas-Melia D, Chauvin F, Deque M, Douville H, Guenou M, Marquet P, Planton S, Royer JF, Tyteca S. 2006. Description and validation of the CNRM-CM3 global coupled model. *Climate Dynamics* (in press).
- Srivastava A, Rajeevan M, Kshirsagar S. 2008. Development of high resolution daily gridded temperature dataset (1969–2000) for Indian region. vol 8, NCC Research Report.
- Tripathi S, Srinivas V, Nanjundiah SR. 2006. Downscaling precipitation for climate change scenarios: a support vector machine approach. *Journal of Hydrology* **330**: 621–640.
- Vrac M, Naveau P. 2007. Stochastic downscaling of precipitation extremes from dry events to heavy rainfalls. *Water Resources Research* **43**: W07405, 13 pp., DOI: 10.1029/2006WR005308.
- Vrac M, Stein M, Hayhoe K. 2007. Statistical downscaling of precipitation through non-homogeneous stochastic weather models. *Climate Research* **34**: 169–184, DOI: 10.3354/cr00696.
- Wilby R, Charles S, Zorita E, Timbal B, Whetton P, Mearns L (eds). 2002. *Guidelines for use of climate scenarios developed from climate models: downscaling methods. Supporting Material of the IPCC*. Working Group II Contribution to the Fourth Assessment Report of the Intergovernmental Panel on Climate Change.
- Wilks D, Wilby R. 1999. The weather generation game: generating realistic weather from a stochastic weather model. *Progress in Physical Geography* **23**: 329–357.
- Wood A, Sridhar V, Lettenmaier D. 2004. Hydrologic implications of climate change: dynamical and statistical approaches to downscaling climate model outputs. *Climate Change* **62**: 189–216.

